Mandible strength and geometry in relation to bite force: a study in three caviomorph rodents

Guido N. Buezas,[1] (iD) Federico Becerra,[1] Alejandra I. Echeverría,[1] (iD) Adrián Cisilino[2] and Aldo I. Vassallo[1] (iD)

[1]*Laboratorio de Morfología Funcional y Comportamiento, Instituto de Investigaciones Marinas y Costeras (IIMyC), Universidad Nacional de Mar del Plata (UNMdP)-Consejo Nacional de Investigaciones Científicas y Técnicas (CONICET), Mar del Plata, Argentina*
[2]*División Mecánica de Materiales, Instituto de Investigaciones en Ciencia y Tecnolgía de Materiales (INTEMA), Universidad Nacional de Mar del Plata (UNMdP)-Consejo Nacional de Investigaciones Científicas y Técnicas (CONICET), Mar del Plata, Argentina*

Abstract

The monophyletic group Caviomorpha constitutes the most diverse rodent clade in terms of locomotion, ecology and diet. Caviomorph species show considerable variation in cranio-mandibular morphology that has been linked to the differences in toughness of dietary items and other behaviors, such as chisel-tooth digging. This work assesses the structural strength of the mandible of three caviomorph species that show remarkable differences in ecology, behavior and bite force: *Chinchilla lanigera* (a surface-dwelling species), *Octodon degus* (a semi-fossorial species) and *Ctenomys talarum* (a subterranean species). Finite element (FE) models of the mandibles are used to predict the stresses they withstand during incisor biting; the results are related to *in vivo* bite forces and interspecific variations in the mandibular geometries. The study concludes that the mandible of *C. talarum* is better able to withstand strong incisor bites. Its powerful adducting musculature is consistent with the notorious lateral expansion of the angular process and the masseteric crest, and the enhanced cortical bone thickness. Although it has a relatively low bite force, the mandible of *O. degus* also shows a good performance for mid-to-strong incisor biting, in contrast to that of *C. lanigera*, which exhibits, from a mechanical point of view, the worst performance. The mandibles of *C. talarum* and *O. degus* appear to be better suited to withstand stronger reaction forces from incisor biting, which is consistent with their closer phylogenetic affinity and shared digging behaviors. The contrast between the low *in vivo* bite force of *C. lanigera* and the relatively high estimations that result from the models suggests that its adductor musculature could play significant roles in functions other than incisor biting.

Key words: Caviomorpha; *Chinchilla*; *Ctenomys*; digging; Finite Element Analysis; mammalian jaw; *Octodon*.

Introduction

The huge diversification in the masticatory apparatus allows vertebrates to access a wide variety of food items. Different taxa process a large variety of foods – in terms of composition and hardness – by means of distinct combinations of jaw adductor muscle configurations, tooth types and dental occlusion mechanics (Hanken & Hall, 1993; Hildebrand & Goslow, 2001; Olivares et al. 2004; Ungar, 2010). Several studies have related bite forces with diet specializations for different vertebrate groups, such as lizards (Herrel & O'Reilly, 2006; Sagonas et al. 2014), finches (Van der Meij & Bout, 2006), spotted hyenas (Binder & Van Valkenburgh, 2000) and bats (Aguirre et al. 2003). Processing hard foods usually requires strong mandibular forces. Muscular forces transmitted through the teeth to the food or other items generate concomitant reaction forces, which must be withstood by the bone structure of the masticatory apparatus. Natural selection is expected to operate both on the attributes involved in the production and transmission of forces and on those that confer structural strength, such as bone architecture and mechanical properties (Currey, 2006; Soons et al. 2015).

Rodents have one of the most specialized masticatory apparatuses. The morphology is primarily related to

Correspondence

Guido N. Buezas, Laboratorio de Morfología Funcional y Comportamiento, Instituto de Investigaciones Marinas y Costeras (IIMyC), Universidad Nacional de Mar del Plata (UNMdP)-Consejo Nacional de Investigaciones Científicas y Técnicas (CONICET), Dean Funes 3350 – 2do piso, (B7602AYJ) Mar del Plata, Prov. Buenos Aires, Argentina.
E: buezasguido@gmail.com

gnawing (the ability to disaggregate hard items through repetitive occlusions with the incisors) and chewing with the molars. Nevertheless, gnawing and chewing functionally exclude one another; because of the different lengths of the diastema in the maxilla and the mandible, incisors and molars cannot occlude simultaneously (Druzinsky, 2015). Rodents have developed a powerful and complex jaw adductor musculature that exerts strong bite forces (Wood, 1965; Hautier et al. 2011). Cranial anatomy and bite forces vary greatly among species due to differences in diet (e.g. Samuels, 2009) and the engagement of incisors in other behaviors and functions, such as digging (Van Daele et al. 2009; Becerra et al. 2011; Becerra, 2015; Van Wassenbergh et al. 2017) and during territory defense and aggressive encounters between males (Vassallo & Busch, 1992; Zenuto et al. 2002; Becerra et al. 2012a).

The infraorder Caviomorpha is probably the most diverse rodent clade in terms of locomotion, ecology and diet (Mares & Ojeda, 1982; Wood, 1985; Ojeda et al. 2015). Species within this infraorder show considerable variation in cranio-mandibular morphology and dental attributes (reviewed by Álvarez et al. 2015). Substantial variation between taxa has been observed for mandible shape and the degree of development of the jaw adductor musculature (Lessa et al. 2008; Álvarez et al. 2011). Becerra et al. (2012b) linked the variations in the incisor bending strength and procumbency to differences in toughness of dietary items and other behaviors, such as chisel-tooth digging. Because of these characteristics, caviomorph rodents constitute an interesting group to investigate how interspecific differences in bite force correlate with the structural strength of the mandibular apparatus.

Simple applications of Newtonian mechanics can supply correct approximations to the mechanics of skeletal structures (Alexander, 1981; Greaves, 1985; Thomason, 1991). The most useful aids for solving a statics problem are free body diagrams (FBD). FBD use simplified geometrical models of skeletal structures and muscular forces to calculate – by means of force and moment equilibrium equations – reactions and internal forces. In the case of the cranio-mandibular system, these are the bite force (reaction force) and forces on the condyle (internal force) (Greaves, 1985; Herrel et al. 1998; Ennos, 2012). FBD are effective for estimating forces and nominal loading modes (tension/compression, shear and/or flexion), but because of the simplified geometrical modeling, they cannot provide accurate estimations for the resulting stress fields. For instance, skull geometries are too complex to attain detailed stress solutions using the FBD approach. An alternative is the direct *in vivo* recording of bone deformations in the skull with strain gauges (Herring & Mucci, 1991; Jaslow & Biewener, 1995; Kopher & Mao, 2003; Sun et al. 2004). This methodology is very precise but cumbersome, as surgery is needed to implant the strain gauges. Moreover, the possible location of gauges on live specimens is limited by factors such as animal size and accessibility to anatomic sites. Over the last decades, Finite Elements Analysis (FEA) has gained attention as a method for understanding the form–function relationships in evolutionary biomechanics (e.g. Richmond et al. 2005; Rayfield, 2007; Kupczik, 2008; Soons et al. 2010; Chalk et al. 2011). FEA uses detailed geometrical models of the skeletal structures – the geometries of which can be obtained by means of non-invasive imaging techniques such as computed tomography (CT) and magnetic resonance imaging (MRI) – to simulate the loadings and compute accurate estimates of the resultant strain and stress fields (Kupczik, 2008; Mazzetta et al. 2009). Nevertheless, the understanding of some structure biomechanics requires the full comprehension of the system (Kupczik, 2008), and FEA is not an exception. It is a powerful tool for complex analyses, but the construction of a model and loading simulations must be compared with results from validated techniques; computational simulation is not a solution *per se*.

This work analyzes the structural strength of the mandibles of three South American rodent species: the surface-dwelling *Chinchilla lanigera* Bennett 1829, the semi-fossorial *Octodon degus* Molina 1782 and the subterranean *Ctenomys talarum* Thomas 1898. These species belong to the monophyletic group Caviomorpha (Upham & Patterson, 2012) though they show important differences in ecology, behavior and bite force. The main characteristics of the three species are summarized below:

- The Talas tuco-tuco *C. talarum* (Caviomorpha: Ctenomyidae) is a small size rodent (bodyweight range in the wild: 110–165 g) that inhabits the south-eastern region of Buenos Aires province in Argentina. It is solitary, subterranean, and lives in self-constructed galleries. It constructs the galleries by digging clayey and hard soils with its forelimbs and incisors, using the incisors to break down the rocks and roots usually present in the burrow path (Vassallo, 1998). The *in vivo* bite force of this species is estimated at 31.7 N (Becerra et al. 2011). As in most ctenomyids, the bite force of Talas tuco-tuco is stronger than expected from its body size due to its hypertrophied masseter muscles (Lessa et al. 2008; Becerra et al. 2011). *Ctenomys* diet is often composed of hard plant items; evidence has been found of frequent damage in stems of the woody shrub *Larrea divaricata* (jarilla) produced by the species *C. mendocinus* in arid environments of the piedmont of Mendoza (Tort et al. 2004). Inter-male encounters are highly aggressive and involve fights with strong bites (Zenuto et al. 2002).
- The common degu *O. degus* (Caviomorpha: Octodontidae) is a semi-fossorial rodent present in central Chile. Its bodyweight in the wild ranges from 170 to 300 g (Woods & Boraker, 1975), which makes it bigger than Talas tuco-tuco. Degu lives in communal burrows that it constructs using the forelimbs. It mainly eats young

leaves of herbs and shrubs, seeds and bark (Woods & Boraker, 1975); very rarely, it uses its slender incisors for cutting roots (Ebensperger, 1998). Because of this diet, the common degu does not need to dig for food. Probably because of its feeding habits and social structure, the *in vivo* bite force of degu (21.9 N; Becerra et al. 2014) is lower than that expected for its body size.

- The long-tailed chinchilla *C. lanigera* (Caviomorpha: Chinchillidae) is native to the rocky and sandy areas of the Andes Mountains. It is a medium size (bodyweight range in the wild: 370–490 g) ground-dweller that shelters within shrubs or in holes between or below rocks (Nowak, 1999; Spotorno et al. 2004). Mainly herbivorous, chinchillas choose to eat plants with more fiber and less lignin content, such as herbs, grasses, sedges, lichens and mosses (Spotorno et al. 2004). The *in vivo* bite force of chinchilla (23.5 N; Becerra et al. 2014) is lower – both, absolutely and relative to its body size – than those of other caviomorph rodents.

Skulls of chisel-tooth digging mammals, such as in *Ctenomys*, are robust and massive (Dubost, 1968). With this regard, Hildebrand (1985) stated that the morphology of digging mammals relates, first, to the need to loosen and move hard materials. These activities require an excavation tool, a transport mechanism to remove the excavated soil, and the skeletal structure and muscles with the capabilities to exercise the various associated forces. Previous studies by the authors (Becerra et al. 2012b) have analyzed the anatomy of the incisors and how this relates to the ability to produce large forces in the subterranean genus *Ctenomys* and allied taxa. Here, we hypothesize that the variation in mandible geometry between the three caviomorph rodents can be explained by the stress levels resulting from interspecific differences in bite force. We expect the more robust mandible of *C. talarum* to show a better relative performance to withstand the stresses generated by incisor biting than those of *O. degus* and *C. lanigera* for equivalent (scaled) load cases. This hypothesis is investigated and tested by means of FE simulations of incisor bites.

Materials and methods

Specimens

The study comprised three adult specimens, one for each species: (1) a tuco-tuco from a natural population inhabiting the grasslands and dune habitats near the coastal village of Mar de Cobo (Buenos Aires Province, Argentina), with a mandible size (i.e. the distance from the condyle to the incisive) of 30.12 mm; (2) a degu provided by the Instituto de Ciencias Ambientales y Evolutivas of the Universidad Austral de Chile (Valdivia, Chile), with a mandible size of 27.10 mm; and (3) a chinchilla obtained from the breeding farm Agro Kaykun in Mar del Plata (Buenos Aires Province, Argentina), with a mandible size of 39.64 mm. Specimens were dissected and their skulls and mandibles cleaned with hot water and detergent;

osteological material is housed in the collection of the Laboratorio de Morfología Funcional y Comportamiento of the Universidad Nacional de Mar del Plata (Mar del Plata, Argentina).

MicroCT scanning and geometry reconstruction

Dry mandibles were scanned using a μCT X-ray scanner (SkyScan 1172, SkyScan/Bruker micro-CT, Kartuizerweg 3B 2550 Kontich, Belgium) at the Laboratório de Técnicas Nucleares da Embrapa Instrumentaçao Agropecuária/CNPDIA (São Carlos, SP, Brazil). Scan parameters were voltage at 100 kV, spot size of 11.38 μm and voxel size of 22.15 μm for the tuco-tuco, and voltage at 59 kV, spot size of 11.31 μm and voxel size of 22.25 μm for both the degu and the chinchilla. SkyScan NRECON v1.6 was used for the reconstructions of the cross-sectional images.

Bone properties

Explorations of the μCT cross-sectional images showed that the mandible consists primarily of cortical bone (see Fig. 1) and cavities, which are either empty or filled with trabecular bone with a very low solid volume fraction. Cortical bone was assumed linear, elastic and isotropic; Young's modulus was measured by means of micro-indentation tests with the Oliver & Pharr (1992) method. Micro-indentations were made on two mandibles of *C. talarum*, which were prepared using the procedure proposed by Ballarre et al. (2011): dry mandibles were fixed in neutral 10 wt% formaldehyde for 24 h, then dehydrated in a series of acetone–water mixtures and in a methacrylated solution, and finally embedded in poly (methyl methacrylate) (PMMA) solution and polymerized. Micro-indentation tests were performed on the diastemas, which were identified from the μCT images as the locations with the highest bone densities. The mandibles embedded in PMMA were cut across the planes C1 (diastema) and C2 (mandibular corpus) (see Fig. 1). Cuts were performed using a low-speed diamond blade saw (Buehler GmbH, Switzerland) cooled with water. Surfaces for the micro-indentations were polished with 600–2000 water-lubricated grid paper and then fine-polished with 0.3 μm alumina powder using an automatic grinding and polishing machine (Logitech, UK). Micro-indentations were made using a TI 900 Triboindenter (Hysitron, Eden Prairie, MN, USA) with a Berkovich indenter. The maximum indentation load was 9000 μN, which was held constant for 30 s to minimize creep effects; loading and unloading rates were at 900 μN s^{-1}. The average of eight micro-indentation tests resulted in a Young's modulus $E = 25.83 \pm 5.15$ MPa, which agrees very well with Rho et al.'s (1997) study on human cortical bone. A value of 0.3 was adopted for the Poisson ratio (Vogel, 2003; Currey, 2006). Following Keyak & Rossi (2000), bone failure was assumed to be the critical yield stress $\sigma_{yc} = 163$ *MPa* (the average between 133 MPa in tension and 193 MPa in compression; data compiled by Currey, 2006). Teeth were assigned the properties of cortical bone. This simplification in tooth material properties is based on the results of Cox et al. (2011), who concluded that tooth material properties have little effect on the strain patterns across the skull in locations other than the teeth themselves.

Muscle forces

The following mandible adductor muscles were considered: superficial masseter (SM), deep masseter (PM), infraorbital zygomatico-mandibularis (ZMIO), zygomaticomandibularis (ZM), temporalis (T),
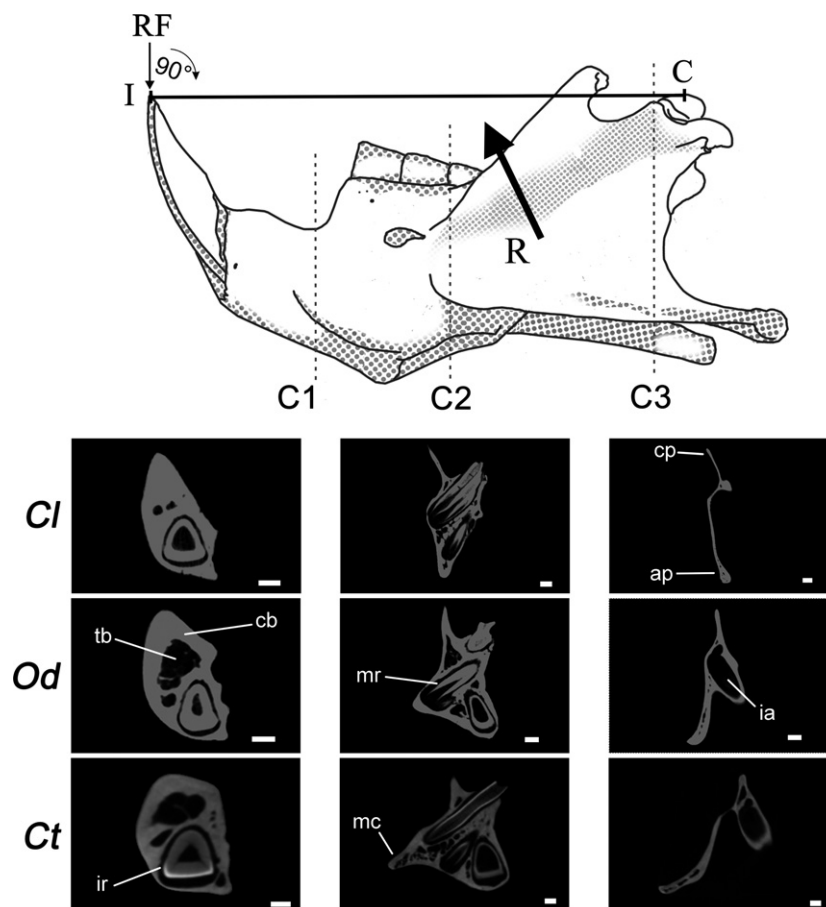
Fig. 1 Schematic representation of a *Ctenomys talarum* mandible in lateral view (above) and bone internal structure of hemimandibles of the studied species (below). Food or soil reaction force (RF) angle is measured with respect to the line between the condyle (C) and the incisor tip (I). R: approximate location of the masticatory muscle's resultant force. The location of the μCT cross-sections is indicated as C_1 (diastema), C_2 (corpus) and C_3 (angular and condyloid process). *Cl*: *Chinchilla lanigera*, *Od*: *Octodon degus*, *Ct*: *Ctenomys talarum*. Left and right sides of cross-sections: lateral and medial side of hemimandible, respectively. ap, angular process; cb, cortical bone; cp, condyloid process; ia, incisor alveolus; ir, incisor root; mc, masseteric crest; mr, molar root; tb, trabecular bone. Scale bar: 1 mm.

posterior extension of the masseter muscle (MXTp) and pterygoideus (Pg). Muscle insertion areas were located as in previous studies on the species by the authors (Becerra et al. 2011, 2014). Muscle lines of action (i.e. the direction from the muscle insertion point to the origin point) were measured directly from specimens using a MicroScribe G2X 3D digitizer. For this purpose, the complete sets of crania and mandibles were articulated for an incisor bite with a gape angle of 10° (see Becerra et al. 2011, 2014). Muscle force moduli, estimated from the physiological cross-sectional area (PCSA) of dissected muscles, were taken from Becerra et al. (2011, 2014); they are reported in Table 1.

Finite element modeling

Geometry reconstruction and finite element discretization

The software AMIRA 5.4 4 (Thermo Fisher Scientific, USA) was used to segment the μCT images and to build the 3D geometry reconstructions and finite element discretizations of the mandibles. Segmented μCT images were then used to build surface meshes of triangles for the mandibles. Based on the observations reported above in section on bone properties, only cavities larger than 0.5 mm were incorporated into the model, and they were assimilated as empty voids; cavities smaller than 0.5 mm and other geometric discontinuities were removed by using automatic and manual geometry repairing tools. Surface meshes were used to discretize the mandibles with 10-node tetrahedral elements (C3D10). The resulting FE discretizations consisted of around 1.2 million elements with a mean element size of 0.2 mm. Finally, the discretizations were imported into ABAQUS v6.12 (Simulia, Johnston, RI, USA) for the finite element model implementation and analysis. FE discretizations were also used to measure the surface area of the mandibles (see Table 1).

It is clearly important to model these variables as accurately as possible in FE models to have the highest possible confidence in the results. Significant variations in material properties were considered and yet the properties of the tooth materials, enamel, dentin and pulp appear to be relatively unimportant in these analyses, despite the large size of the incisors in rodents, and can be varied widely with little effect on the overall pattern of deformation across the skull. Nevertheless, these variables can have a substantial influence locally and, of course, are paramount when studying deformation in the teeth themselves.

Table 1 Muscle input forces from anatomical dissections, scaled to the *in vivo* bite forces (in italics).

	Muscle input forces (N)							Model surface area (mm²)	Bite force (N)	
	SM	PM	MXTp	ZMIO	ZM	T	Pg		FEM 1	FEM 2
Chinchilla lanigera	17.44	24.21	3.74	14.99	9.67	6.32	17.32	3492.7	21.23	65.34
	6.1	*8.47*	*1.31*	*5.25*	*3.39*	*2.21*	*6.06*			
Octodon degus	9.18	16.46	2.23	8.23	9.67	6.99	4.71	2458.2	20.02	40.52
	6.42	*11.53*	*1.56*	*5.76*	*4.18*	*4.89*	*3.3*			
Ctenomys talarum	18.03	23.55	4.06	11.19	13.97	8.31	10.64	2040.3	32.43	
	12.62	*16.49*	*2.84*	*7.83*	*9.78*	*5.82*	*7.45*			

MXTp, posterior extension of the masseter muscle; Pg, pterygoideus; PM, deep masseter; SM, superficial masseter; T, temporal; ZM, zygomaticomandibularis; ZMIO, infraorbital zygomaticomandibularis. Bite forces; FEM 1, bite forces adjusted to match *in vivo* values; FEM 2, resultant bite forces from models with muscle forces scaled to those of *C. talarum* (see Materials and methods). Muscle forces taken from anatomical dissections (Becerra et al. 2011, 2014).

Boundary conditions

Rodent mandibles during incisor biting can be assimilated to a third-class lever, in which the resultant of the adductor input forces (R in Fig. 1) is between the bite output force at the incisors (RF at point I in Fig. 1) and the temporomandibular joint (the fulcrum). The incisor bite forces were computed assuming the simultaneous activation of all adductor muscles at both sides of the jaw (symmetric bites). FE models were set up as follows. Temporo-mandibular joints were modeled by restricting all displacement of the nodes at the center of curvature of the condyle surfaces. Muscle forces were applied as distributed forces on their insertion areas. The displacement of the node at the incisor tip on the sagittal plane (point I on the in Fig. 1) was restricted in the direction perpendicular to the plane that contains the condyles and the incisor tip. This configuration results in the maximum bite force (Becerra et al. 2014).

The abovementioned data for mandible geometries, muscle forces and boundary conditions were also used to make estimations of the bite forces by means of three-dimensional FBD models (Ozkaya & Nordin, 1999). FBD models are similar to that used in Becerra et al. (2014) and were based on the computation of the static force equilibrium, in which muscles' moment across the jaw joint equals the food or soil reaction force moment (Becerra et al. 2014).

Load cases

Two load cases were considered. In the first load case, the mandibles are loaded with their corresponding adductor forces to compute the bite forces and the mandibular safety factor of each of the species. Safety factors were computed as the quotients between the critical yield stress and the local von Mises stress, $SF = \sigma_{yc}/\sigma_{VM}$, at nine locations on the mandibles: labial and lingual regions at the protrusion of the incisors, the diastema, the region between the coronoid process and the molar row, the region below the condyle, the mandibular corpus, the region between the condyloid and coronoid processes, the masseteric crests, and the region between the condyloid and angular processes. These regions are labeled from R1 to R9 and their anatomical positions are indicated in Fig. 2.

In a second load case, models for the chinchilla and the degu were loaded with the scaled adductor muscle forces of the tuco-tuco to compare mandible performances in terms of their robustness-to-lightness ratios. Scaled adductor input forces for the chinchilla and the degu were determined using the method of Dumont et al. (2009). Based on the assumptions that stress governs failure and that stress is directly proportional to force and inversely
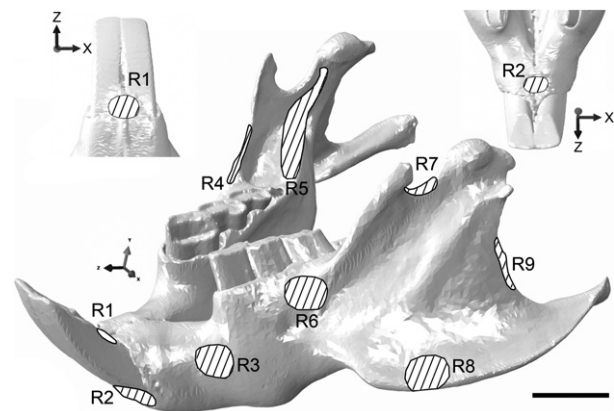

Fig. 2 Reconstruction of the mandible of *Ctenomys talarum* with schematic identification of the nine regions for which stress and SF values are reported in Table 3. R1 and R2, dorsal and ventral incisor-tooth protrusions (see details in dorsal and ventral views, respectively); R3, mandible diastema; R4, region between coronoid process and molar row; R5, region below condyle (medially); R6, mandibular corpus; R7, region between condyloid and coronoid processes; R8, masseteric crest; R9, region between condyloid and angular processes. Scale bar: 5 mm.

proportional to area, Dumont et al. (2009) propose removing the effects of size between two models by scaling muscle forces such that the force per unit surface area is kept constant. Thus, any differences between the stress and strain fields of the models will be entirely due to their differences in shape. Suppose we have the results of two finite element models, *A* and *B*, of different shapes and surface areas (S_A and S_B) that have been loaded with total force values F_A and F_B, respectively. To match their force/surface area ratios, one can scale the force applied to model *B* to create a new model, *B'*, with the applied force

$$F_{B'} = \left(\frac{S_B}{S_A}\right)F_A$$

Based on the surface area data reported in Table 1, the scale factors for adductor forces of tuco-tuco when applied to the

chinchilla and the degu are $\left(\frac{S_{chinchilla}}{S_{tuco-tuco}}\right) = 1.712$ and $\left(\frac{S_{degu}}{S_{tuco-tuco}}\right) = 1.205$, respectively.

Results

Mandible geometries

Shape and internal structures of the three mandibles were compared by inspection of the μCT images. Figure 1 depicts the cross-sections of the mandibles at the levels of the diastema (C1), the mandibular corpus (C2) and the angular process (C3). Table 2 reports the data of the cross-section aspect ratios (i.e. the quotient dorso-ventral length: medio-lateral length) and average cortical bone thicknesses (the quotient cortical bone cross-section area : external perimeter). It is observed that the three mandibles are dorso-ventrally elongated; the maximum elongations are always found for the chinchilla, and the minimum elongations for the tuco-tuco. It is also interesting to observe that whereas chinchilla and degu present the maximum elongation at the condyle (section C3), the maximum elongation of tuco-tuco is at the diastema (C1). In terms of the cortical bone thickness, the three species present their maxima at the diastema. Extreme cases are the tuco-tuco – which has the widest and most massive diastema, and the mandibular corpus and the angular process with an exceptional lateral expansion – and the chinchilla – whose angular process is almost vertically orientated. Note that the incisor alveoli of the tuco-tuco and the degu extend up to the condylar process (Fig. 1 C$_3$), but it much shorter for the chinchilla.

Bite forces

Incisor bite forces that resulted of the first load case are 54.05 N for the tuco-tuco, 28.6 N for the degu, and 53.08 N for the chinchilla. These bite force estimations differ by around 8% with respect to those of the FBD models; differences are attributed to discrepancies in the positions of the muscle insertions (note that muscle insertions are areas in the FE model, whereas they are points in the FBD model). The position of the overall muscle force resultant is located at 31% of the mandible length for the tuco-tuco, and at 36% for the degu and the chinchilla. These values are close to the theoretical estimate proposed by Greaves (1982, 2012) that the muscle resultant should be positioned at one-third of the jaw length to ensure a mechanically stable configuration.

As for previous analyses by the authors (see Becerra et al. 2011, 2014), bite force results of the FE models overestimate the *in vivo* measurements by 71% for the tuco-tuco, 31% for the degu and 126% for the chinchilla. These discrepancies could be mainly explained by experimental uncertainties associated to the *in vivo* measurement of bite forces. It should be considered that there is always a motivational factor that might affect the observations when *in vivo* performances or physiological parameters are under study; it is therefore not possible to guarantee that the animals exerted their maximum bite forces during the experiments reported by Becerra et al. (2014). Other sources of variation, probably of less relative importance, are hypotheses concerning the simultaneous activation of all adductor muscles (Weijs, 1994; Langenbach & van Eijden, 2001) and the estimation of the muscle forces from the PCSA. Nevertheless, uncertainties associated with the locations of the muscle insertion areas and the muscle force directions are considered low, as they were measured directly from the specimens.

Based on the above considerations, discrepancies between the computed and *in vivo* bite forces were associated to the overestimation of the muscle forces. Therefore, muscle forces were proportionally and equally reduced for each of the three species until the bite forces of the FE models matched their *in vivo* counterparts. The resulting bite forces are reported in column FEM 1 of Table 1.

Bite forces of the second load case (i.e. the degu and the chinchilla loaded with the scaled adductor forces of the tuco-tuco) are reported in column FEM 2 of Table 1. Note

Table 2 Aspect ratios (dorso-ventral length : medio-lateral length) and average cortical bone thickness (cortical bone area: external perimeter) of the mandible cross-sections (see Fig. 1).

	Chinchilla lanigera		*Octodon degus*		*Ctenomys talarum*	
	Cross-section aspect ratio	Cortical bone thickness (mm)	Cross-section aspect ratio	Cortical bone thickness (mm)	Cross-section aspect ratio	Cortical bone thickness (mm)
Diastema (C1)	1.72	0.48	1.51	0.57	1.29	0.86
Mandibular corpus (C2)	1.91	0.54	1.22	0.60	0.86	0.54
Angular and condyloid process (C3)	5.18	0.19	2.48	0.33	1.18	0.42

Aspect ratios > 1 indicate the dorso-ventral elongation of the mandibles.

that whereas the bite force of the degu and the chinchilla are nearly identical for load case 1, the bite force of the chinchilla exceeds that of degu by 50% for load case 2.

Stress analysis

Simulations showed that, in agreement with the third-class lever model described in the section on boundary conditions, the general stress pattern is compatible with that of a beam bending in the sagittal plane. Tension and compression zones are easily distinguished in sagittal and coronal planes across the diastema of the tuco-tuco in Fig. 3.

Stress results of the two load cases are reported in Fig. 4 and Table 3. Figure 4 depicts the contour plots for the von Mises' stresses and Table 3 reports the von Mises' stress values and safety factors for the nine regions across the mandible (see Fig. 2).

Results of *load case 1* (FEM 1, Table 3) show that the three species present the same overall stress pattern across the mandible: the highest stress levels are exhibited by the narrowest bone sections, such as the regions between the coronoid processes and the molar rows (R4), below the condyles (R5), between the condyles and the coronoid processes (R7) and the masseteric crests (R8). The thickest sections, such as the regions of teeth (R1 and R2), the diastema (R3) and the mandibular corpus (R6), also exhibit the lowest stress levels. Von Mises' stress patterns across the mandible of the three species indicate that the ascending ramus tends to present high stress levels, whereas the mandibular corpus experiences relatively low stresses (see Fig. 4).

Results of *load case 2* show substantial differences in stress distributions with respect to those of *load case 1*: the chinchilla and the degu show notable increases in the surface area subjected to high stresses, which now spread through the ascending ramus. In the case of the chinchilla, high stress areas also extend to the diastema (Fig. 4). Stress levels for the chinchilla increase from around 2.5 times in the angular process (regions R8 and R9) to approximately 3.6 times in the diastema (R3) and below the condyle (R5) (see Table 3). The stress level for the degu is roughly double that of *load case 1* (see Table 3).

Discussion

Consistent with the third-class lever model mentioned above, mandible cross-sections are dorso-ventrally elongated and medio-laterally compressed, which suggests greater resistance to bending in the sagittal plane (Fig. 1, Table 2). The same pattern is also found in felids, for which the mandibular corpus depths are double the mandible widths underneath the cheek teeth (Biknevicius & Ruff, 1992; Therrien, 2005). These authors explained the dorso-ventral elongation of the mandible shape as an adaptation to the powerful canine biting used by felids to hold and kill their prey, an interpretation that is comparable to the strong incisor biting by rodents. Moreover, rodent mandibles have an arch-like shape in lateral view, which may enhance its bending strength (Vassallo, 2016).

The three species present the same overall bone thickness pattern: bone thicknesses in the diastemas and the mandibular corpuses are, in general, greater than in the ascending ramus (Fig. 1). But, in combination with this general pattern, there are also significant local variations in the thickness of different regions of the mandibles. These local thickness variations are identified as the main explanation for the important differences – of up to an order of magnitude – in the stress values between different locations in the mandible (Table 3). Broadly, the von Mises' stress patterns of the three mandibles (see Fig. 4) match those of squirrels, guinea pigs and rats in Cox & Jeffery (2015). These authors found that the posterior part of the mandibles (the region around the condylar and the angular processes) tends to present high stress levels, whereas the zone surrounding and ventral to the molar alveoli experiences relatively lower stresses. Bone distribution and mandible geometry can have significant effects on stress produced by mastication, even at an intraspecific level. A study on the development of the masticatory apparatus in rabbits (*Oryctolagus cuniculus*) found that masticatory peak stresses associated with hard diets resulted in increases of mandibular proportions (e.g. corpus height and width) and increased biomineralization of the temporomandibular joint surface (Ravosa et al. 2010).
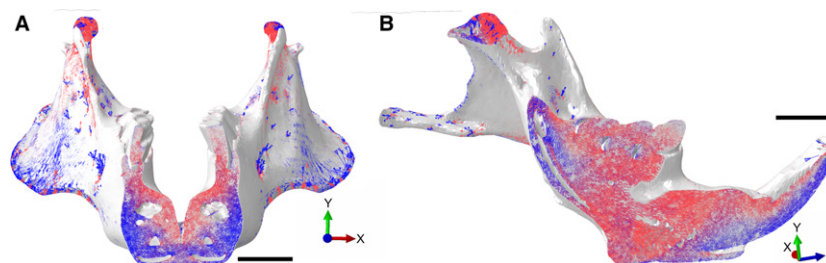

Fig. 3 Maximum (related to tension, in red) and minimum (related to compression, in blue) principal stresses over coronal (a) and sagittal (b) sections of a *Ctenomys talarum* mandible. Note that the general stress pattern is compatible with that of a beam bending on the sagittal plane. Scale bar: 5 mm.
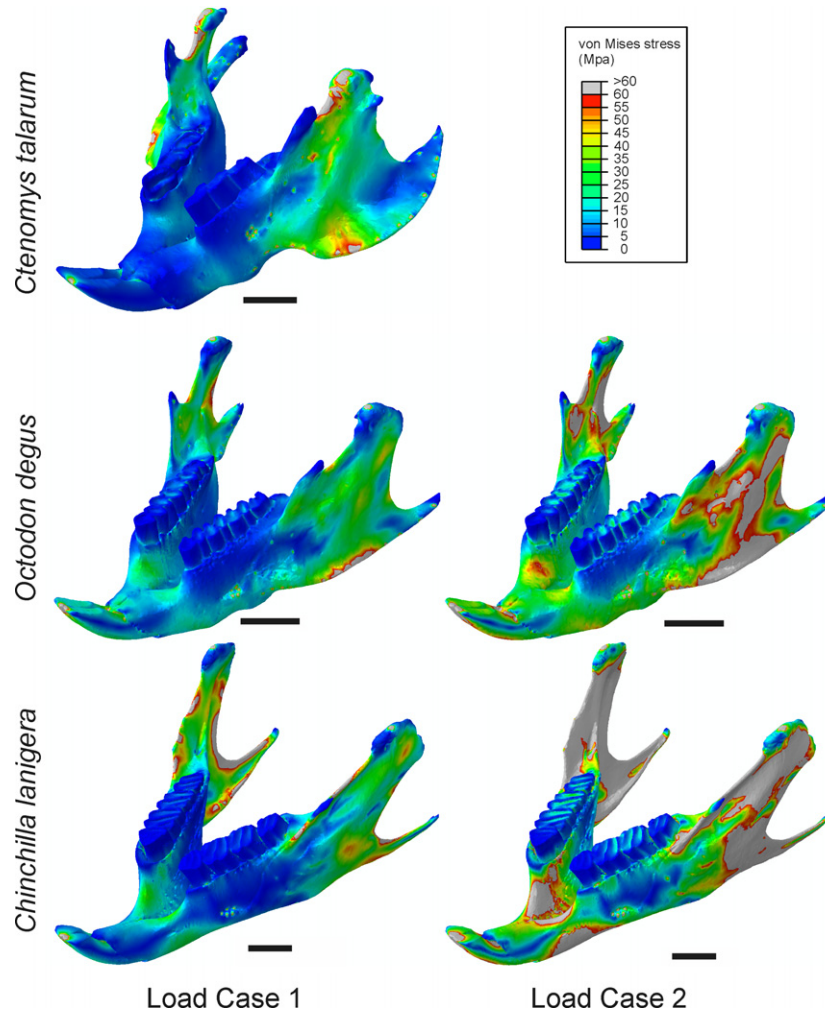
Fig. 4 Von Mises' stress contour plots for the three species and the two *load cases*. The same color map is used for the five plots, where warmer colors depict higher von Mises stresses. An arbitrary threshold of 60 MPa is used to better illustrate the stress gradients on the mandibles. Scale bar: 5 mm.

The notorious lateral expansion of the angular process and the masseteric crest of the tuco-tuco stands out when comparing the shapes of the three mandibles (Fig. 1). These are linked to an increase of the attachment site area for the hypertrophied masseteric musculature of the family Ctenomyidae (Verzi, 2002; Lessa et al. 2008). This characteristic – which has also been observed in extant and fossil ctenomyid species (e.g. Reig & Quintana, 1992; Vassallo, 1998) – is related to the use of the incisors as digging tools and to the high bite force of tuco-tucos.

Stress results for the biting analyses (*load case 1*) show that the mandibles of the three species present analogous spatial distributions of the SF (see Table 3): minimum values are spread over the zone of the ascending ramus and masseteric crest (R4, R5, R7, R8, and R9), whereas maximum values are at the mandibular corpus (R6). It can be argued that the safe factor concept makes no sense for regions with high values of SF; let us say SF values of 6.8, 28.1 and 26.3 at

R3 for chinchilla, degu and tuco-tuco, respectively, indicate that bone will not break at the diastemas. However, SFs are effective for comparison with the structural performances of the mandibles and to recognize the regions that are more sensitive to the changes in the load configuration.

Condyles and angular processes have a relatively homogeneous distribution of SFs for the three species, with minimum values ranging from 1.8 to 5.5. SF maxima occur at the mandibular corpuses, in agreement with Vassallo's (2016) findings. SF maxima for tuco-tuco and degu are 2–2.5 times higher than for chinchilla (Table 3). The large amount of bone necessary to hold the deep-rooted molars of tuco-tucos, degus and chinchillas can explain the maximum SFs at the mandibular corpus. It remains an open question whether the high SF values at the mandibular corpus are related to hypsodonty, a condition shared by the studied species that refers to the possession of high-crowned teeth with prolonged or continuous generation of

Table 3 Von Mises' stress (in MPa) and safety factors (SF) in nine regions across the mandible for the bite forces of *load cases 1* and *2* (FEM 1 and FEM 2; see Table 1).

| | FEM 1 | | | | | | FEM 2 | | | |
| | *Chinchilla lanigera* | | *Octodon degus* | | *Ctenomys talarum* | | *C. lanigera* | | *O. degus* | |
Region	Stress	SF	Stress	SF	Stress	SF	Stress	SF	Stress	SF
R1	16.8	9.7	27.7	5.9	9.7	16.8	51.7	3.2	56.1	2.9
R2	18.5	8.8	27.2	6.0	6.5	25.1	57	2.9	55	3.0
R3	23.8	6.8	5.8	28.1	6.2	26.3	85.1	1.9	11.6	14.1
R4	58.2	2.8	24.9	6.5	21.2	7.7	174.4	0.9	49.3	3.3
R5	36.9	4.4	40.7	4.0	29.7	5.5	131.8	1.2	86.6	1.9
R6	8.1	20.1	3.9	41.8	3.3	49.4	23.9	6.8	8.1	20.1
R7	70.1	2.3	39	4.2	66.7	2.4	240	0.7	89.4	1.8
R8	39.3	4.1	72.7	2.2	52.8	3.1	90.7	1.8	158	1.0
R9	90.3	1.8	54.1	3.0	29.6	5.5	239.9	0.7	111.8	1.4

SFs were computed using a critical yield stress of 163 MPa. See Fig. 2 for the identification of regions R1–R9.

dental tissue. Hypsodonty and open-rooted cheek teeth have evolved several times in rodents and other mammals as an adaptation to abrasive diets (Janis, 1988; von Koenigswald et al. 1994; Verzi et al. 2004).

As for the mandibular corpuses, the SFs at the diastema of degu and tuco-tuco are markedly higher (around four times) than in chinchillas. In contrast, chinchilla and degu present similar SFs at the incisor zone, whereas the SF of tuco-tuco is markedly greater. The higher structural strength of the diastema and incisor zone of tuco-tucos is compatible with the mechanical resistance necessary to withstand the repeated load due to chisel-tooth digging. Continuous pressure on the surrounding bone can be very high during the use of incisors for digging: for the blind mole-rat *Spalax*, there is evidence that loads transmitted by the incisors lead to cell and tissue fatigue, resulting in damage of the palatal bone in aged individuals (Zuri & Terkel, 2001). SF values at the incisor zone in degus and chinchillas are within the same order of magnitude as those reported by Thomason & Russell (1986) for the rostral region of a didelphid marsupial (range 1.8–11.0), and the value of 7 reported by Alexander (1981) for the mandible of a primate species.

The stress levels of the degu and the chinchilla for *load case 2* present an overall increase with respect to *load case 1*. Consistent with the increase in the stress level, *load case 2* results in a general reduction of the SF, but regions with extreme values of the SFs remain in the same locations of *load case 1* (the maximum values are at the mandibular corpuses and the lowest values are spread over the ascending ramus). It is interesting to note that regions within the ascending ramus of chinchilla – R4, R7 and R9 – have SF < 1, that is, the mandible of chinchilla would not be capable of withstanding the scaled muscle forces of tuco-tuco. The feasible bite force for the chinchilla under these conditions is estimated to be 45.78 N, which results from the product of the bite force computed for this load case (65.34 N; Table 1) times the minimum SF (0.7 at R7 and R9; Table 3). In contrast to the chinchilla, the increase of the stress level of the degu for *load case 2* is more homogeneous across the mandible, with stresses roughly double those of the *load case 1* (Table 3). Consistent with the increase in the stress levels, SFs are around half those in the *load case 1*, being the maximum and minimum (in the limit of the bone failure) values at the mandibular corpus and masseteric crest, respectively. Results for the *load case 2* show that, when loaded with the scaled muscle forces of the tuco-tuco, the structural strength of the mandible in the degu is greater than in the chinchilla, which indicates that the degu is able to withstand stronger incisor biting.

In agreement with results of previous works by Becerra et al. (2011, 2014), models overestimate the *in vivo* bite force measurements. One cause of these discrepancies is the impossibility of guaranteeing that the animals exert their maximum biting forces during the experiments (Davis et al. 2010). Moreover, the studied species vary in the level of aggressiveness and this affects the experimental measurements of bite force (Becerra et al. 2014). Another issue is that the modulation of the fiber recruitment pattern can substantially vary muscle activation and the resulting output (Cleuren et al. 1995; Herring, 2007). Additional FE analyses to assess the stresses generated by the muscles when acting independently could be used to refine the models. It is interesting to link the analysis for the bite force estimations with the degree of adaptation of a species for incisor biting. Chinchillas – which present the lowest records of incisor biting – show the greatest overestimation of the bite force based on muscle PCSA,

whereas the overestimations for tuco-tucos and degus – which are better adapted for incisor biting – are substantially lower. Thus, the adductor musculature of chinchillas could play a significant role in functions other than incisor biting, such as chewing with oblique mandibular movements, unilateral occlusion and asymmetric contraction of the jaw musculature (Olivares et al. 2004) to process hard vegetal items. On other hand, the relatively lower overestimation of bite forces for tuco-tucos and degus is consistent with the more central role that incisor biting plays in their digging and feeding behaviors.

In summary, our observations and results show that the mandible of tuco-tucos appears to be better suited than those of degu and chinchilla to withstand the stresses generated by strong incisor biting. Although it has a relatively low bite force, the mandible of degu shows an adequate performance for mid-to-strong incisor biting. The chinchilla exhibits, from a mechanical point of view, the worst performance. The three species belong to the monophyletic group Caviomorpha, but although the subterranean tuco-tuco and the semi-fossorial degus are phylogenetically close (they belong to the sister families Ctenomyidae and Octodontidae, respectively), they are relatively distant from the ground-dweller chinchilla (Upham & Patterson, 2012). This indicates that the better performance in incisor biting of tuco-tucos and degus could be a shared derived characteristic.

Conclusions

This work studies the relative structural strengths of the mandibles of *C. lanigera*, *O. degus* and *C. talarum* for incisor biting. The study comprises FE simulations to estimate the stress experienced by the mandibles when loaded with the forces exerted by their adductor musculature and when loaded with the scaled muscle forces of other species. The latter analysis allows the mandibular performances to be compared in terms of their robustness-to-lightness ratios.

The results of the study support our initial assertion about the capability of FE stress analyses to relate the interspecific differences in bite force with variations in mandible geometries. The three mandibles are dorso-ventrally elongated and medio-laterally compressed (which favors the resistance to bending in the sagittal plane), and bone in the diastemas and the mandibular corpuses are much thicker than in the ascending ramus. Interspecific variations of these patterns lead to the differences between the structural performances of the three mandibles.

We conclude that the mandible of tuco-tuco is better able to withstand strong incisor bites. Its powerful adductor musculature is consistent with the enhanced mandible robustness in the diastema and the angular process, which has direct effects upon the reduction of the stress level at these regions. This feature results in a jaw architecture with the capability to perform strong bites with a high safety factor.

Author contributions

G.N.B. and A.I.V.: conceived the research; G.N.B.; F.B.; A.I.E. and A.I.V.: acquisition of data; G.N.B. and A.C.: data analysis; G.N.B.; A.I.V. and A.C.: drafting of the manuscript. All authors provided critical revision of the manuscript and approval of the article.

References

Aguirre LF, Herrel A, Van Damme R, et al. (2003) The implications of food hardness for diet in bats. *Funct Ecol* **17**, 201–212.

Alexander RM (1981) Factors of safety in the structure of animals. *Sci Prog* **67**, 109–130.

Álvarez A, Pérez SI, Verzi DH (2011) Ecological and phylogenetic influence on mandible shape variation of South American caviomorph rodents (Rodentia: Hystricomorpha). *Biol J Linn Soc* **102**, 828–837.

Álvarez A, Vieytes EC, Becerra F, et al. (2015) Diversity of craniomandibular morphology in caviomorph rodents: an overview of macroevolutionary and functional patterns. In: *Biology of Caviomorph Rodents: Diversity and Evolution* (eds Vassallo AI, Antenuchi CD), pp. 199–228. Buenos Aires: SAREM Sociedad Argentina para el Estudio de los Mamíferos.

Ballarre J, Seltzer R, Mendoza E, et al. (2011) Morphologic and nanomechanical characterization of bone tissue growth around bioactive sol–gel coatings containing wollastonite particles applied on stainless steel implants. *Mater Sci Eng* **31**, 545–552.

Becerra F (2015) *Aparato masticatorio en roedores caviomorfos (Rodentia: Hystricognathi): Análisis morfo-funcional con énfasis en el género Ctenomys (Ctenomyidae)*. PhD Thesis, Universidad Nacional de Mar del Plata.

Becerra F, Echeverría AI, Vassallo AI, et al. (2011) Bite force and jaw biomechanics in the subterranean rodent Talas tuco-tuco (*Ctenomys talarum*) (Caviomorpha: Octodontoidea). *Can J Zool* **89**, 334–342.

Becerra F, Echeverría AI, Marcos A, et al. (2012a) Sexual selection in a polygynous rodent (*Ctenomys talarum*): an analysis of fighting capacity. *Zoology* **115**, 405–410.

Becerra F, Echeverría AI, Vassallo AI, et al. (2012b) Scaling and adaptations of incisors and cheek teeth in caviomorph rodents (Rodentia, Hystricognathi). *J Morphol* **273**, 1150–1162.

Becerra F, Echeverría AI, Casinos A, et al. (2014) Another bites the dust: bite force and ecology in three caviomorph rodents (Rodentia, Hystricognathi). *J Exp Zool* **321**, 220–232.

Biknevicius AR, Ruff CB (1992) The structure of the mandibular corpus and its relationship to feeding behaviours in extant carnivorans. *J Zool* **228**, 479–507.

Binder W, Van Valkenburgh B (2000) Development of bite strength and feeding behaviour in juvenile spotted hyenas (*Crocuta crocuta*). *J Zool* **252**, 273–283.

Chalk J, Richmond BG, Ross CF, et al. (2011) Finite Element Analysis of masticatory stress hypotheses. *Am J Phys Anthropol* **145**, 1–10.

Cleuren J, Aerts P, De Vree FL (1995) Bite and joint force analysis in *Caiman crocodilus. Belg J Zool* **125**, 79–94.

Cox PG, Jeffery N (2015) The muscles of mastication in rodents and the function of the medial pterygoid. In: *Evolution of the Rodents: Advances in Phylogeny, Functional Morphology and Development* (eds Cox P, Hautier L), pp. 350–372. Cambridge: Cambridge University Press.

Cox PG, Fagan MJ, Rayfield EJ, et al. (2011) Finite element modelling of squirrel, guinea pig and rat skulls: using geometric morphometrics to assess sensitivity. *J Anat* **219**, 696–709.

Currey JD (2006) *Bones, Structure and Mechanics.* Princeton: Princeton University Press.

Davis JL, Santana SE, Dumont ER, et al. (2010) Predicting bite force in mammals: two-dimensional versus three-dimensional lever models. *J Exp Biol* **213**, 1844–1851.

Druzinsky RE (2015) The oral apparatus of rodents: variations on the theme of a gnawing machine. In: *Evolution of the Rodents: Advances in Phylogeny, Functional Morphology and Development* (eds Cox P, Hautier L), pp. 323–349. Cambridge: Cambridge University Press.

Dubost G (1968) Les mammiferes souterrains. *Rev D'écol Biol Sol* **5**, 99–133.

Dumont ER, Grosse IR, Slater GJ (2009) Requirements for comparing the performance of finite element models of biological structures. *J Theor Biol* **256**, 93–103.

Ebensperger LA (1998) Sociality in rodents: the New World fossorial hystricognaths as study models. *Rev Chil Hist Nat* **71**, 65–77.

Ennos R (2012) Balance, angular momentum and sport. *Phys World* **25**, 31–34.

Greaves WS (1982) A mechanical limitation on the position of the jaw muscles of mammals: the one-third rule. *J Mammal* **63**, 261–266.

Greaves WS (1985) The mammalian postorbital bar as torsion-resisting helical strut. *J Zool* **207**, 125–136.

Greaves WS (2012) *The Mammalian Jaw: A Mechanical Analysis.* Cambridge: Cambridge University Press.

Hanken J, Hall BK (1993) *The Skull (Vol. 3: Development).* Chicago: Chicago University Press.

Hautier L, Lebrun R, Saksiri S, et al. (2011) Hystricognathy vs sciurognathy in the rodent jaw: a new morphometric assessment of hystricognathy applied to the living fossil *Laonastes* (Diatomyidae). *PLoS ONE* **6**, e18698.

Herrel A, O'Reilly JC (2006) Ontogenetic scaling of bite force in lizards and turtles. *Physiol Biochem Zool* **79**, 31–42.

Herrel A, Aerts P, De Vree F (1998) Static biting in lizards: functional morphology of the temporal ligaments. *J Zool* **244**, 135–143.

Herring SW (2007) Masticatory muscles and the skull: a comparative perspective. *Arch Oral Biol* **52**, 296–299.

Herring SW, Mucci RJ (1991) *In vivo* strain in cranial sutures: the zygomatic arch. *J Morphol* **207**, 225–239.

Hildebrand M (1985) Digging of quadrupeds. In: *Functional Vertebrate Morphology* (eds Hildebrand M, Bramble DM, Liem KF, Wake DB), pp. 89–109. Cambridge: The Belknap Press of Harvard University Press.

Hildebrand M, Goslow G (2001) *Analysis of Vertebrate Structure.* 5th edn. New York: John Wiley and Sons.

Janis CM (1988) An estimation of tooth volume and hypsodonty indices in ungulate mammals, and the correlation of these factors with dietary differences. In: *Teeth Revisited: Proceedings of the VII International Symposium on Dental Morphology*, Vol. 53 (eds Russell DF, Santoro JP, Sigogneau-Russell D), pp. 367–387. Paris: Mémoire Museum National d'Histoire Naturelle.

Jaslow CR, Biewener AA (1995) Strain patterns in the horncores, cranial bones and sutures of goats (*Capra hircus*) during impact loading. *J Zool* **235**, 193–210.

Keyak JH, Rossi SA (2000) Prediction of femoral fracture load using finite element models: an examination of stress- and strain-based failure theories. *J Biomech* **33**, 209–214.

von Koenigswald W, Martin Sander P, Leite MB, et al. (1994) Functional symmetries in the schmelzmuster and morphology of rootless rodent molars. *Zool J Linn Soc* **110**, 141–179.

Kopher RA, Mao JJ (2003) Suture growth modulated by the oscillatory component of micromechanical strain. *J Bone Miner Res* **18**, 521–528.

Kupczik K (2008) Virtual biomechanics: basic concepts and technical aspects of finite element analysis in vertebrate morphology. *J Anthropol Sci* **86**, 193–198.

Langenbach GEJ, van Eijden TMGJ (2001) Mammalian feeding motor patterns. *Am Zool* **41**, 1338–1351.

Lessa EP, Vassallo AI, Verzi DH, et al. (2008) Evolution of the morphological adaptation for digging in living and extinct ctenomyid and octodontid rodents (Rodentia: Caviomorpha: Octodontoidea). *Biol J Linn Soc* **95**, 267–283.

Mares M, Ojeda R (1982) Patterns of diversity and adaptation in South American hystricognath rodents. In *Mammalian Biology in South America* (eds Mares MA, Genoways HH), pp. 393–430. Pittsburgh: Pymatuning Laboratory of Ecology, University of Pittsburgh.

Mazzetta GV, Cisilino AP, Blanco E, et al. (2009) Cranial mechanics and functional interpretation of the horned carnivorous dinosaur *Carnotaurus sastrei. J Vert Paleont* **29**, 822–830.

Nowak RM (1999) *Walker's Mammals of the World II.* 6th edn. Baltimore: The Johns Hopkins University Press.

Ojeda RA, Novillo A, Ojeda AA (2015) Large-scale richness patterns, biogeography and ecological diversification in caviomorph rodents. In: *Biology of Caviomorph Rodents: Diversity and Evolution* (eds Vassallo AI, Antenuchi CD), pp. 121–138. Buenos Aires: SAREM Sociedad Argentina para el Estudio de los Mamíferos.

Olivares AI, Verzi DH, Vassallo AI (2004) Masticatory morphological diversity and chewing modes in South American caviomorph rodents (Octodontidae). *J Zool* **263**, 267–277.

Oliver WC, Pharr GM (1992) An improved technique for determining hardness and elastic modulus using load and displacement sensing indentation experiments. *J Mater Res* **7**, 1564–1583.

Ozkaya N, Nordin M (1999) *Fundamentals of Biomechanics.* Berlin: Springer Verlag.

Ravosa MJ, Ning J, Costley DB, et al. (2010) Masticatory biomechanics and masseter fiber-type plasticity. *J Musculoskelet Neuronal Interact* **10**, 46–55.

Rayfield E (2007) Finite Element Analysis and understanding the biomechanics and evolution of living and fossil organisms. *Annu Rev Earth Planet Sci* **35**, 541–576.

Reig OA, Quintana CA (1992) Fossil ctenomyine rodents of the genus *Eucelophorus* (Caviomorpha: Octodontidae) from the

Pliocene and Early Pleistocene of Argentina. *Ameghiniana* **29**, 363–380.

Rho JY, Tsui TY, Pharr GM (1997) Elastic properties of human cortical and trabecular lamellar bone measured by nanoindentation. *Biomaterials* **18**, 1325–1330.

Richmond GB, Wright BW, Grosse I, et al. (2005) Finite element analysis in functional morphology. *Anat Rec A* **238**(A), 259–274.

Sagonas K, Pafilis P, Lymberakis P, et al. (2014) Insularity affects head morphology, bite force and diet in a Mediterranean lizard. *Biol J Linn Soc* **112**, 369–484.

Samuels JX (2009) Cranial morphology and dietary habits of rodents. *Zool J Linn Soc* **156**, 864–888.

Soons J, Herrel A, Genbrugge A, et al. (2010) Mechanical stress, fracture risk, and beak evolution in Darwin's ground finches (Geospiza). *Philos Trans R Soc* **365**, 1093–1098.

Soons J, Genbrugge A, Podos J, et al. (2015) Is beak morphology in Darwin's Finches tuned to loading demands? *PLoS ONE* **10**, e0129479.

Spotorno AE, Zuleta CA, Valladares JP, et al. (2004) *Chinchilla lanigera*. *Mamm Spec* **758**, 1–9.

Sun Z, Lee E, Herring SW (2004) Cranial sutures and bones: growth and fusion in relation to masticatory strain. *Anat Rec A* **276**, 150–161.

Therrien F (2005) Mandibular force profiles of extant carnivorans and implications for the feeding behavior of extinct predators. *J Zool* **267**, 249–270.

Thomason JJ (1991) Cranial strength in relation to estimated biting forces in some mammals. *Can J Zool* **69**, 2326–2333.

Thomason JJ, Russell AP (1986) Mechanical factors in the evolution of the mammalian secondary palate: a theoretical analysis. *J Morphol* **189**, 199–213.

Tort J, Campos C, Borghi C (2004) Herbivory by tuco-tucos (*Ctenomys mendocinus*) on shrubs in the upper limit of the Monte desert (Argentina). *Mammalia* **68**, 15–21.

Ungar P (2010) *Mammal Teeth: Origin, Evolution, and Diversity*. Baltimore: Johns Hopkins University Press.

Upham NS, Patterson BD (2012) Diversification and biogeography of the Neotropical caviomorph lineage Octodontoidea (Rodentia: Hystricognathi). *Mol Phylogenet Evol* **63**, 417–429.

Van Daele PAAG, Herrel A, Adriaens D (2009) Biting performance in teeth-digging African mole-rats (Fukomys, Bathyergidae, Rodentia). *Physiol Biochem Zool* **82**, 40–50.

Van der Meij MA, Bout RG (2006) Seed husking time and maximal bite force in finches. *J Exp Biol* **209**, 3329–3335.

Van Wassenbergh S, Heindryckx S, Adriaens D (2017) Kinematics of chisel-tooth digging by African mole-rats. *J Exp Biol* **220**, 4479–4485.

Vassallo AI (1998) Functional morphology, comparative behavior, and adaptation in two sympatric subterranean rodents genus *Ctenomys* (Caviomorpha: Octodontidae). *J Zool* **244**, 415–427.

Vassallo AI (2016) Analysis of arch-like bones: the rodent mandible as a case study. *J Morphol* **277**, 879–887.

Vassallo AI, Busch C (1992) Interspecific agonism between two sympatric species of *Ctenomys* (Rodentia: Octodontidae) in captivity. *Behaviour* **120**, 40–50.

Verzi DH (2002) Patrones de evolución morfológica en Ctenomyinae (Rodentia, Octodontidae). *J Neotrop Mammal* **9**, 309–328.

Verzi DH, Vieytes EC, Montalvo CI (2004) Evolutionary pattern of molars in the *Xenodontomys* phyletic sequence and first notice on secondary acquisition of radial enamel in rodents (Rodentia, Caviomorpha, Octodontidae). *Geobios* **37**, 795–806.

Vogel S (2003) *Comparative Biomechanics: Life's Physical World*. Princeton: Princeton University Press.

Weijs WA (1994) Evolutionary approach of masticatory motor patterns in mammals. In: *Advances in Comparative and Environmental Physiology* (eds Bels V, Chardon M, Vandewalle P), pp. 282–320. Berlin: Springer-Verlag.

Wood AE (1965) Grades and clades among rodents. *Evolution* **19**, 115–130.

Wood AE (1985) The relationships, origin, and dispersal of hystricognath rodents. In: *Evolutionary Relationships among Rodents, a Multidisciplinary Approach* (eds Luckett WP, Hartenberger JR), pp. 475–513. New York: Plenum Press.

Woods CA, Boraker DK (1975) *Octodon degus*. *Mamm Spec* **67**, 1–5.

Zenuto R, Vassallo AI, Busch C (2002) Comportamiento social y reproductivo del roedor subterráneo solitario *Ctenomys talarum* (Rodentia: Ctenomyidae) en condiciones de semicautiverio. *Rev Chil Hist Nat* **75**, 165–177.

Zuri I, Terkel J (2001) Reversed palatal perforation by upper incisors in ageing blind mole-rats (*Spalax ehrenbergi*). *J Anat* **199**, 591–598.